

COMITATO NAZIONALE PER L'ENERGIA NUCLEARE
Laboratori Nazionali di Frascati

LNF-72/98

15 Novembre 1972

A. Balzarotti, L. Bartolini, A. Bianconi, E. Burattini, M. Grandolfo,
R. Habel and M. Piacentini : ULTRAVIOLET SPECTROSCOPY
USING SYNCHROTRON RADIATION.

LNF-72/98
15. Novembre 1972

A. Balzarotti^(x), L. Bartolini, A. Bianconi^(x), E. Burattini^(x),
M. Grandolfo^(o), R. Habel, M. Piacentini^(x): ULTRAVIOLET
SPECTROSCOPY USING SYNCHROTRON RADIATION.

ABSTRACT -

The radiation emitted by the 1.1 GeV synchrotron of the Frascati National Laboratories has been utilized as source of extreme ultraviolet light for physical experiments. The main features of this source are described and the experimental equipment built to perform absorption measurements on solids in the photon energy range 50 - 220 eV is analyzed. The absorption spectra of various metal thin films are presented and discussed.

-
- (x) - Istituto di Fisica dell'Università di Roma and Gruppo Nazionale di Struttura della Materia del C. N. R. - Sezione di Roma, Italy.
(o) - Laboratori di Fisica, Istituto Superiore di Sanità, Roma - Italy.

2.

1. - INTRODUCTION -

The radiation emitted by the electrons accelerated in electron synchrotrons and storage rings has been used in the last years as an intense continuum source for researches in molecular and solid state spectroscopy in the vacuum ultraviolet and soft X-ray spectral ranges. A review of extreme ultraviolet spectroscopy has been recently written by Goodwin⁽¹⁾ and the great variety of the physical and technical problems arising in such spectral range can be found in recent conference and meeting reports⁽²⁾.

Because of its peculiar features, mainly those arising from its high intensity and degree of polarization, the interest in synchrotron radiation is still increasing in several laboratories. In this paper we present a detailed description of the facility available at the Frascati Laboratories of CNEN. The first programs utilizing the radiation emitted by the electron synchrotron started in early 1962 with studies on photoemission cross sections in thin metallic films⁽³⁾. The activity grew when a new group began its efforts to perform optical investigations on solids⁽⁴⁾ and this line of research is now expanding. After a brief discussion of the unique properties of the radiation source, made in Sect. 2, we describe the experimental apparatus in Sect. 3. In Sect. 4 we report on our results for the spectral distribution of the radiation and on the absorption of several metal thin films in the wavelength range 50-200 Å.

2. - PRINCIPAL CHARACTERISTICS OF THE RADIATION EMITTED BY THE FRASCATI SYNCHROTRON. -

The main properties of the radiation emitted by the electrons accelerated in the Frascati electron synchrotron have been already reported in detail elsewhere⁽⁵⁾. We summarize here the main characteristics of the radiation, and analyze in detail those features which are interesting for the design of an optical apparatus not generally encountered with conventional sources.

The number $N(\lambda, E)$ of photons of wavelength λ , radiated per second and per unit bandwidth by each monoenergetic electron of energy E orbiting in the Frascati machine, is represented by

$$(1) \quad N(\lambda, E) = 1.74 \times 10^7 E^4 G(y) \quad (\text{phot.}/\text{Å} \cdot \text{sec})$$

where $G(y)$ is a universal function containing the electron energy E (expressed in GeV) through the parameter $y = \lambda_c / \lambda_0$. $\lambda_c = 20.12/E^3$ corresponds to the cutoff of the spectral distribution at short wavelengths.

However, since the electrons are continuously accelerated from their injection energy to the maximum energy, the spectral distribution of the light changes during the acceleration time. The spectral distribution which should be considered as typical of synchrotron is therefore obtained by integrating the instantaneous distribution $N(\lambda, E)$ over the entire acceleration cycle T according to:

$$(2) \quad \langle N(\lambda) \rangle = \frac{1}{T} \int_0^T N(\lambda, E) dt$$

In Fig. 1 the spectral distributions calculated for both monoenergetic electrons of 1 GeV from eq. (1) and for electrons accelerated up to 1 GeV from eq. 2 are compared. The effect of the integration is that of lowering the intensity of the source and of shifting the maximum of the spectrum, λ_{\max} to smaller energies. This wavelength shift is due to the dependence of λ_{\max} , which decreases as E^{-3} with increasing electron energy, according to $\lambda_{\max} = 0.7 \lambda_c$.

The number of photons per second per \AA utilized by an optical apparatus is not simply the function $\langle N(\lambda) \rangle$ times the number of electrons in orbit. Horizontal and vertical oscillations of the electron beam, known as betatron oscillations, spread the electrons on a beam of finite width. Although this situation deteriorates the ideal picture of a point radiating source, it never is a serious drawback due to the small dimensions (some millimeters) of the bunch.

The photon flux collected by a vertical slit s of width w located at a distance d from the light source (the slit may be the entrance slit of the monochromator) is given by

$$(3) \quad \Phi(\lambda) = \langle N(\lambda) \rangle \cdot n \cdot F \quad (\text{phot. / } \text{\AA} \text{ sec})$$

where n is the number of electrons in the beam and $F = w/2\pi d$ is the geometrical factor expressing the fraction of power entering the slit. In writing eq. (3) we made the assumption that all the vertical distribution of the radiation is collected, in distinction to a conventional source. In fact the synchrotron radiation is emitted in the form of a narrow cone pointing in the forward direction whose axis is tangent to the instantaneous velocity of the electron. Since the aperture of this cone is small (about 0.5 mrad at $E = 1$ GeV), the light intensity drops rapidly within a few milliradians in the direction normal to the orbit plane. Fig. 2 gives the angular distribution of the radiation emitted from monoenergetic electrons of 1 GeV at three different wavelengths. The curves have been calculated using the equation(6)

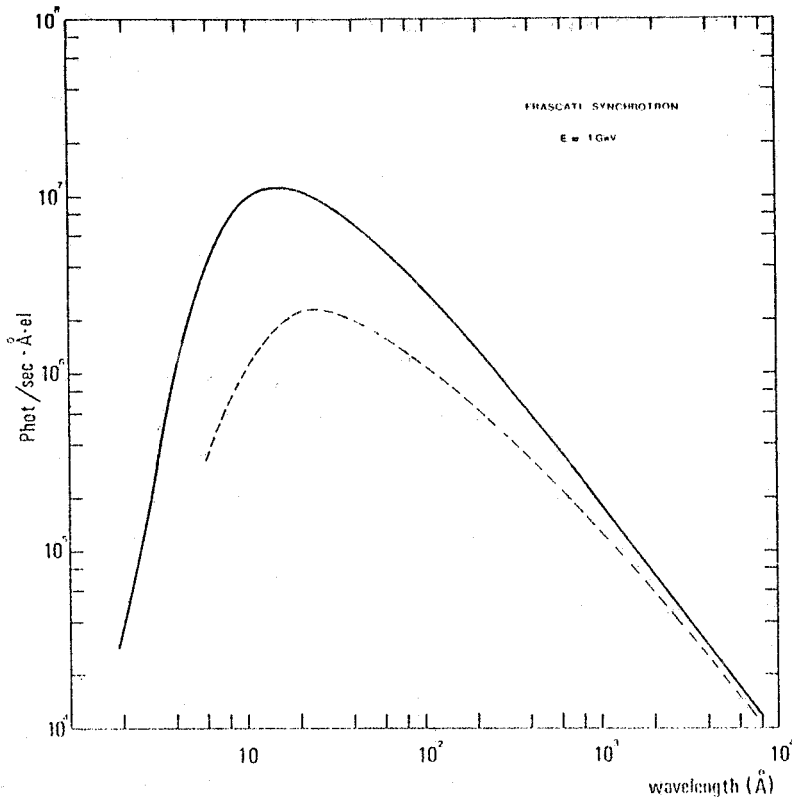


FIG. 1 - Spectral distribution of the radiation emitted by electrons orbiting in the Frascati electronsynchrotron. Full line: monoenergetic electrons of 1 GeV. Broken line: integrated spectrum for electrons accelerated up to 1 GeV.

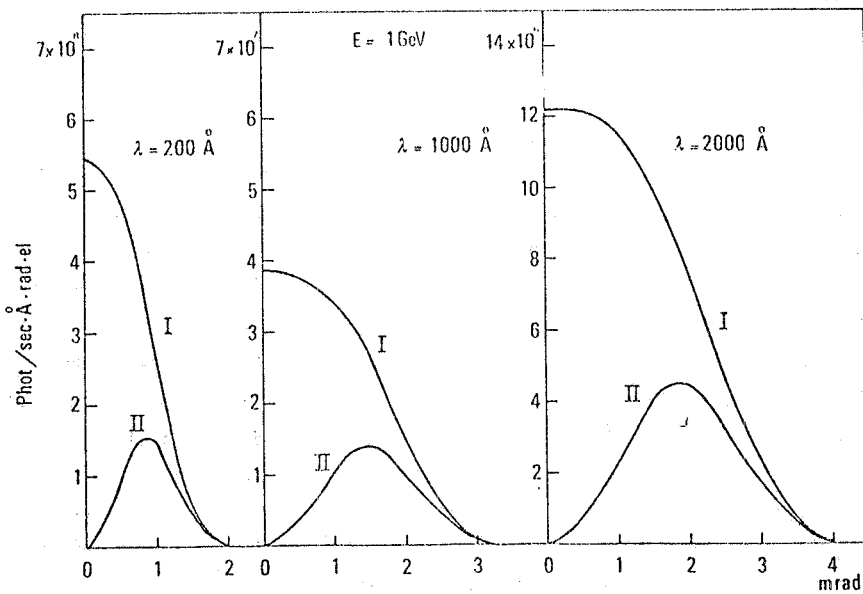


FIG. 2 - Angular distribution of the radiation for three different wavelengths at the maximum energy of the machine.

$$(4) \quad N(\lambda, \psi, E) = 0.89 \cdot 10^{10} E^5 y^3 (1+x^2)^2 \left[K_{2/3}^2(\xi) + \frac{x^2}{1+x^2} K_{1/3}^2(\xi) \right]$$

where ψ is the azimuthal angle measured with respect to the orbit plane, $x = (E/m_0 c^2) \psi$ and $\xi = y/2 (1+x^2)^{3/2}$. $K_{2/3}$ and $K_{1/3}$ are modified Bessel functions of second kind. The two terms in square brackets give the contributions arising from the two components of polarization of the light with the electric field parallel and perpendicular to the orbit plane respectively. The degree of polarization P of the light

$$(5) \quad P(\psi) = \frac{N_{\parallel} - N_{\perp}}{N_{\parallel} + N_{\perp}} = \frac{K_{2/3}^2 + x^2 \left[K_{2/3}^2(\xi) - K_{1/3}^2(\xi) \right]}{K_{2/3}^2 + x^2 \left[K_{2/3}^2(\xi) + K_{1/3}^2(\xi) \right]}$$

is therefore ψ -dependent. For $\psi = 0$ the light is completely linearly polarized with the electric field lying in the orbit plane. For small values of ψ the light is elliptically polarized, while at larger elevations it becomes circularly polarized.

In calculating the actual spectral distributions of the light collected by the slit and its degree of polarization, one has to take into account the height z of the slit. Suppose that the slit is symmetrical with respect to the electron orbit and define χ as the azimuthal angle of observation seen from the slit ($\chi = z/2d \approx 1$ mrad in our arrangement). Fig. 2 shows that the assumption of collecting all the vertical distribution holds only at short wavelengths. Therefore the spectral distribution to be considered is represented by

$$\mathcal{N}(\lambda, E) = \frac{1}{2\chi} \int_{-\chi}^{+\chi} N(\lambda, E, \psi) d\psi$$

instead of eq. (1). In Fig. 3 we show the result of such calculation performed for both components of polarization. The degree of polarization must now be defined as $\mathcal{P} = (\mathcal{N}_{\parallel} - \mathcal{N}_{\perp}) / (\mathcal{N}_{\parallel} + \mathcal{N}_{\perp})$ and it is given in Fig. 4 vs. wavelength. Apart from the initial decrease of the degree of polarization marking the transition from linear to elliptical polarization, the general trend of P is a continuous slight increase with increasing wavelength. This is due to the fact that the ratio between the observation angle χ and the cone aperture ψ decreases with increasing

6.

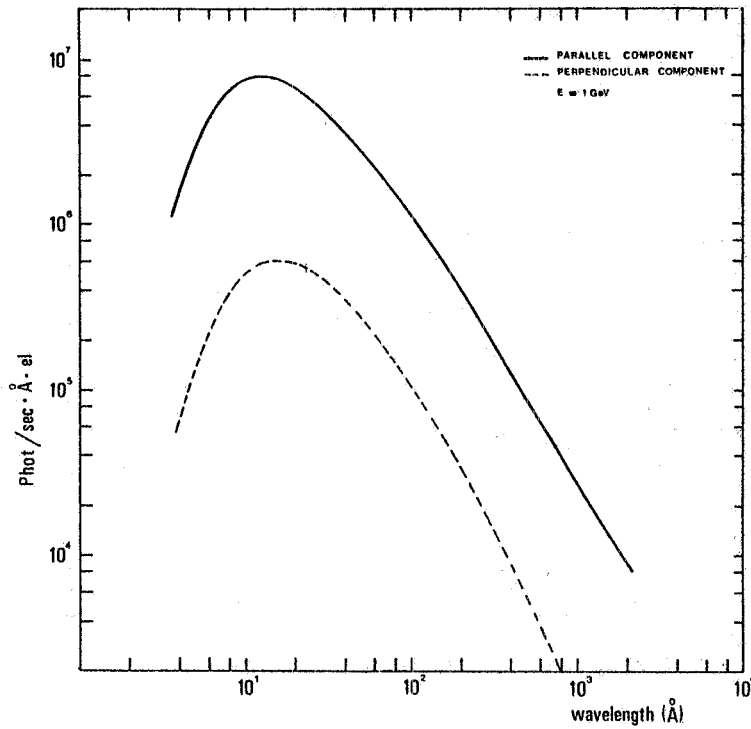


FIG. 3 - Spectral distribution for the two polarization components (parallel and perpendicular to the orbit plane) integrated over an angular aperture of 2 mrad symmetrical with respect to the orbit plane.

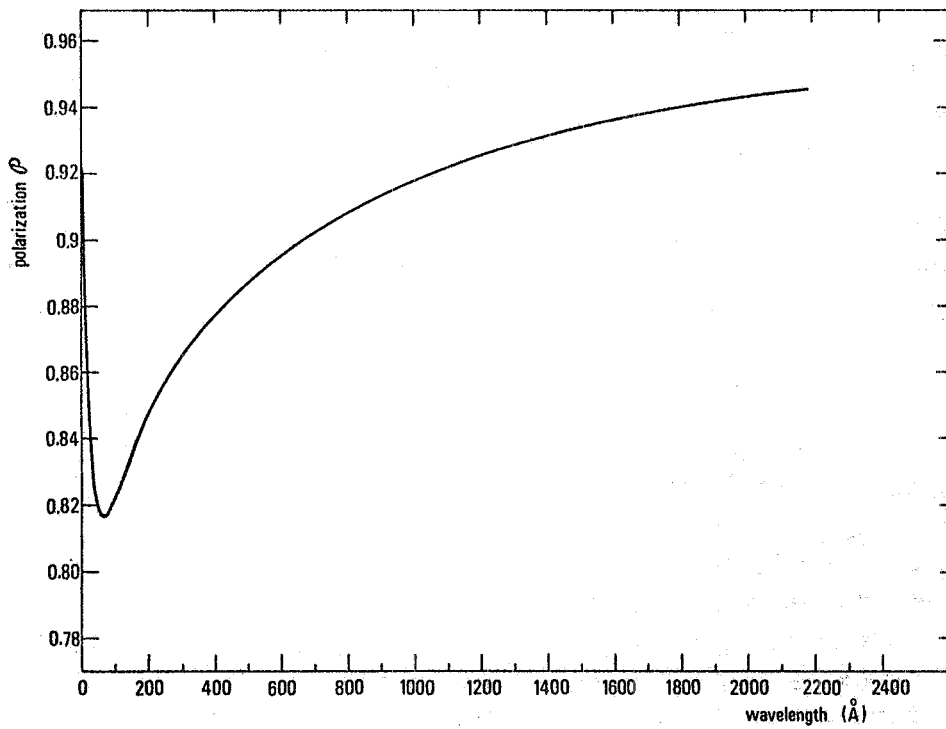


FIG. 4 - Degree of polarization of the radiation vs wavelength.

wavelength, approximating more and more the condition of observation in the orbit plane.

3. - EXPERIMENTAL LAYOUT. -

The Frascati synchrotron radiation facility, shown in Fig. 5, has been designed so that far ultraviolet measurements practically do not interfere with high energy physics experiments and that, in so far as possible, the inverse is also true. The experimental set-up is composed of four major sections:

- i) the synchrotron doughnut,
- ii) the high vacuum system,
- iii) the grazing incidence monochromator,
- iv) the experimental chamber.

A radiation port is arranged at the synchrotron doughnut so that light from a curved section of the electron path can be utilized. The accelerated electrons are grouped in space in four bunches and losses due to light emission are made up by a 43.5 MHz radio-frequency cavity. Because of lack of windows beyond the LiF limit (1050 Å), the entire optical apparatus is open to the electron synchrotron vacuum chamber, which is continuously evacuated by means of oil diffusion pumps in the pressure range of 10^{-7} torr. The access to the doughnut is provided by a 50 mm diameter stainless steel pipe some 7 m long. Both manual and quick closing electropneumatic valves assure that the synchrotron will not be exposed to any vacuum break and allow to separate the system in four distinct sections.

The light pipe, the monochromator and the experimental chamber are evacuated by three independent ion pumps, to an ultimate vacuum better than 10^{-7} . The roughing system is provided by cryosorption pumps and by a turbomolecular pump, which has to be stopped during the measurements in order to avoid vibrations of the spectrometer. In fig. 6 a complete diagram of the vacuum system is shown.

The vacuum uv monochromator is a 2.2 m grazing incidence, Mc Pherson model 247 and conforms to a Rowland circle mounting for concave gratings. The entire system is mounted on a granite base which provides a dimensionally stable base for the optics. A non-scanning slit assembly normally works as the entrance slit and can be moved with respect to the grating along the curved way for setting angles of incidence from 82° to 88° in steps of 0.5° . At present we set the angle of incidence at 86° . The grating is gold coated, has 600 grooves/mm and a ruled area of 53 x 30 mm and it is blazed with an angle of $2^\circ 4'$. The wavelength scanning is performed moving the exit slit, and consequently the experimental chamber, along a curved stainless steel way

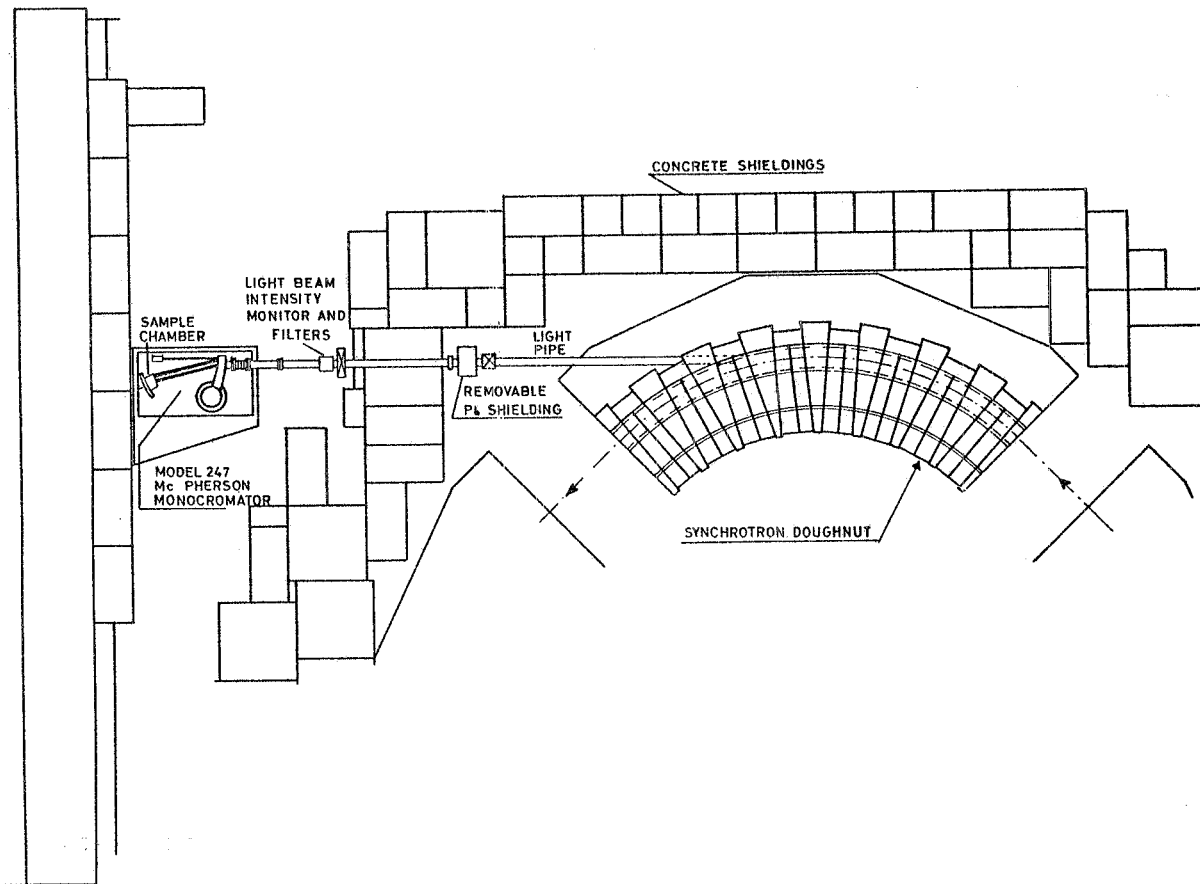


FIG. 5 - Diagram of the synchrotron radiation facility for spectroscopy measurements in the 50 - 250 Å range.

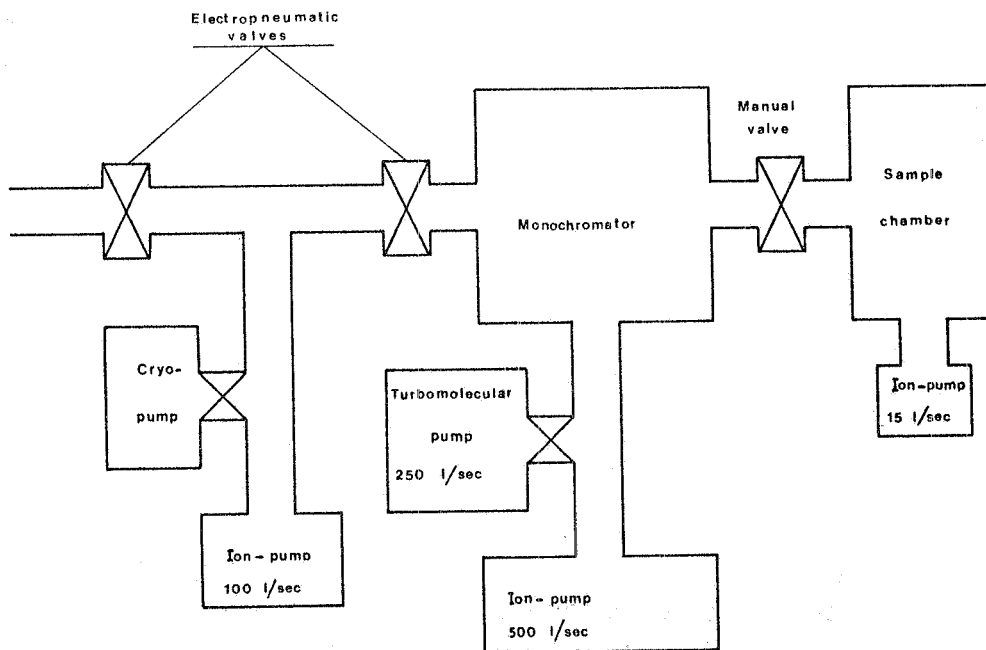


FIG. 6 - Schematic block diagram of the vacuum system.

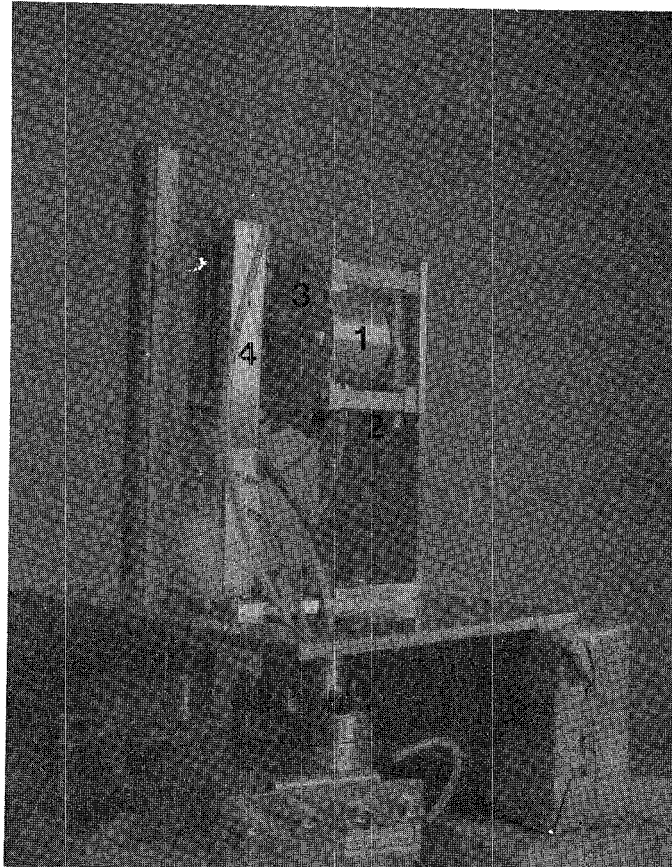


Fig.7

machined to the Rowland circle radius.

The experimental chamber is equipped with a system providing the instantaneous normalization between the incident light and that transmitted through the sample. The samples are mounted on a wheel as shown in Fig. 7. This wheel rotates synchronously with the light pulses so that one pulse goes through the sample while the next pulse goes directly into the detector. The phase adjustment between light pulses and windows is achieved by means of a phase motor which rotates the synchronous one on its axis. The radiation is detected by means of a Bendix M-306 windowless magnetic electron multiplier with a tungsten cathode. The output of the Bendix is amplified by a Sanborn mod. 8865A dc differential amplifier and fed to the inputs of two boxcar integrators PAR CW-1, whose internal trigger is driven through a binary flip-flop synchronous with the machine. In this way a complete separation of alternative pulses in the two channels is achieved. The two signals are finally integrated over a large number of pulses in order to avoid errors arising from the fluctuations of the electron beam intensity. The outputs of the boxcars are fed into a digital ratiometer (HP model 3450 A) giving directly the transmittance of the samples. This transmission is converted in analog form and displayed on an X-Y chart recorder. We have started a program to record the signals in digital form on the magnetic tape of an on-line computer Laben 70. The magnetic tape is then processed by an IBM 360/44 computer. In Fig. 8 a schematic block diagram of the electronics is shown.

4. - EXPERIMENTAL RESULTS AND DISCUSSION. -

The synchrotron radiation spectrum as measured at the sample position in the range 50-270 Å is presented in Fig. 9. The light intensity is given in arbitrary units; however a rough estimate of the photon flux present at the exit slit of the monochromator can be made. For the Frascati synchrotron the beam intensity is approximately 10^{10} electrons/pulse and the repetition rate is 20 pulse/sec of about 20 msec duration. In these conditions the average number of electrons per second in orbit is $5 \cdot 10^9$. According to (3), the photon flux entering the monochromator when $w = 100\mu$ is $\Phi(\lambda) = 10^4 N(\lambda)$ phot./Å sec. If the vertical distribution collected is within 2 mrad, $N(\lambda) = 10^6$ phot./Å sec from Fig. 3, and therefore $\Phi = 10^{10}$ phot./Å sec at 100 Å. At this wavelength the reciprocal linear dispersion of the monochromator is about 1 Å/mm, giving a bandwidth of 0.1 Å in the working conditions. If the loss factor of the monochromator is assumed to be 10^{-2} , the number of photons/sec coming out from the exit slit is about 10^7 .

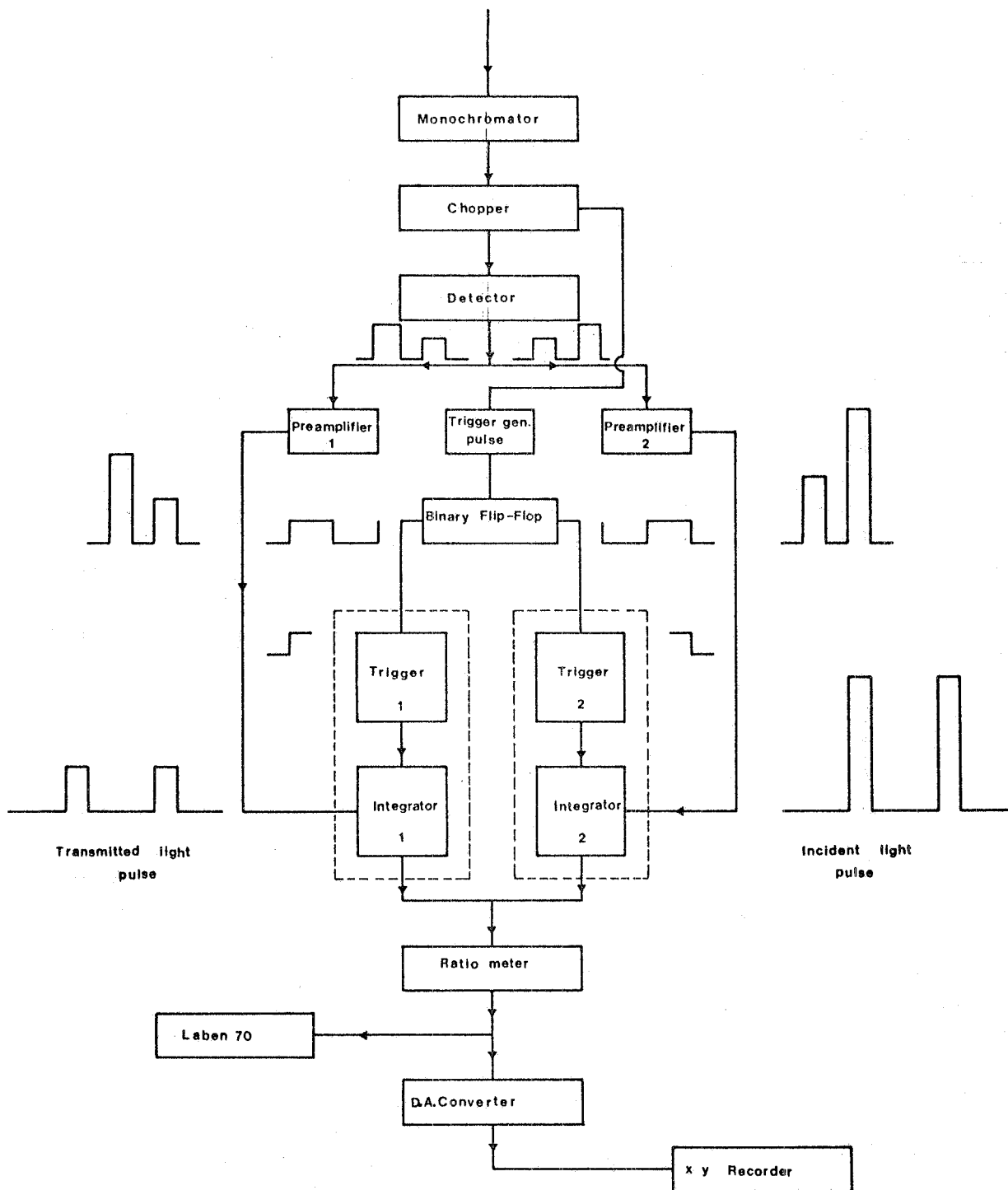


FIG. 8 - Schematic block diagram of the electronic system.

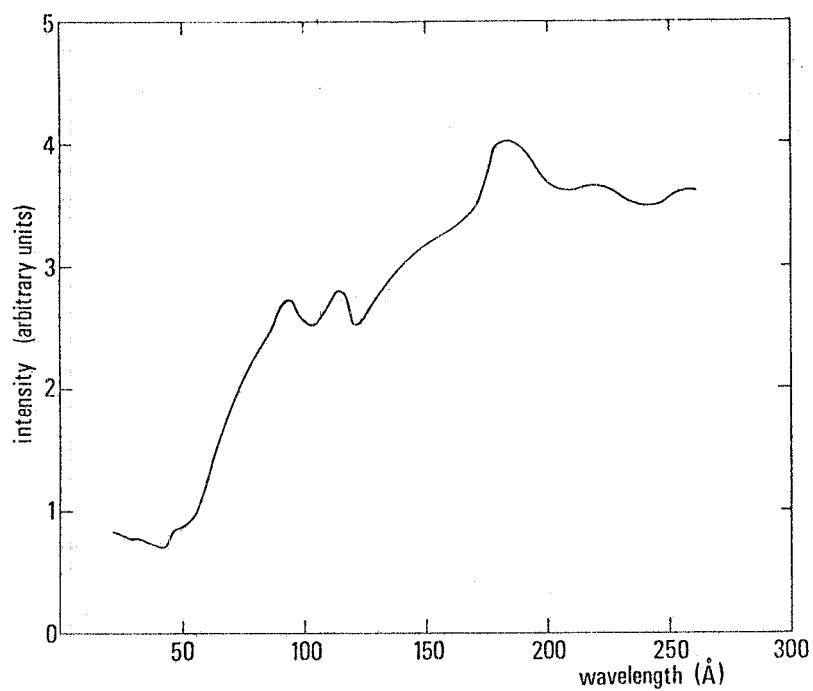


FIG. 9 - Spectral distribution of the synchrotron radiation measured at the exit slit of the grazing incidence Mc Pherson monochromator model 247 with a magnetic electron multiplier Bendix M - 306.

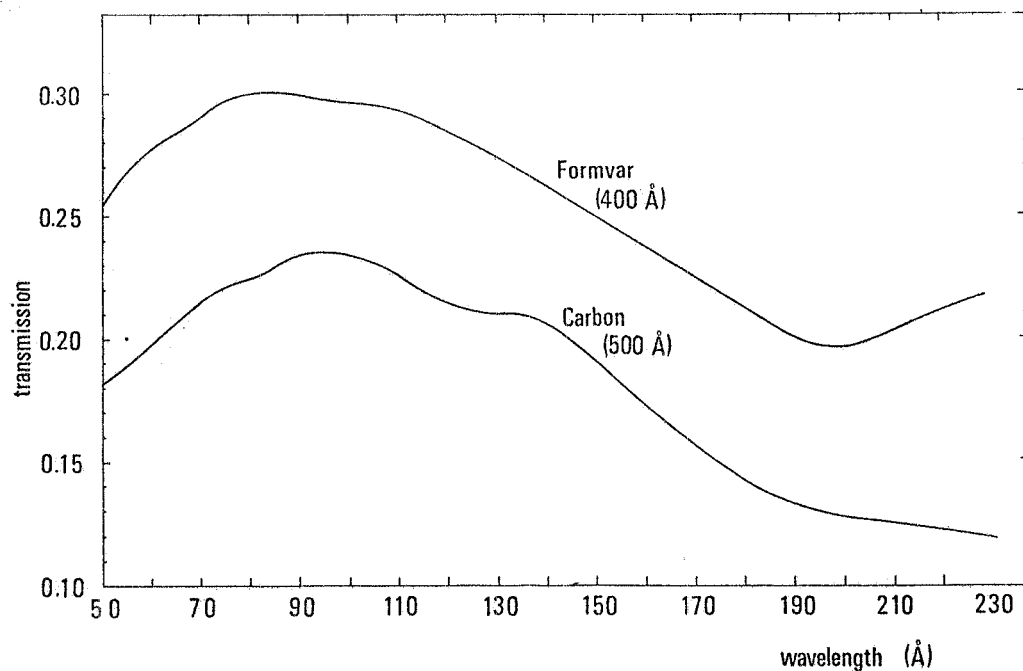


FIG. 10 - Transmission of Formvar and Carbon films in the spectral range 50 - 220 Å.

The spectrum of Fig. 9 is the combined spectral response of the grating and of the detector. The grating efficiency increases in correspondence of the blaze wavelength (120 Å) producing an enhancement of the intensity signal at this wavelength. Second order structures appear above 120 Å, while pure first order light is useful in the 50-120 Å range.

To reduce the second order intensities, suitable transmission filters can be used. For this purpose we have studied the transmittance of thin films of several materials in the region of interest and the results are shown in Fig. 10 and Fig. 11. Some of them (e. g. formvar and carbon⁽⁷⁾) are used as substrates for other materials, which can not be supported.

The transmission of carbon, of formvar and of gold are in good agreement with those measured by Gäwiller et al.⁽⁸⁾ in the same spectral range. Indium and gold are efficient windows between 70 and 110 Å for reducing the stray light specularly reflected by the grating.

In order to check the performance of our apparatus, we measured the absorption coefficient of an aluminium film. The spectrum, shown in Fig. 12, was taken without filters and with a resolution better than 0.1 Å. The energies of the prominent structures are in good agreement with those found in literature and are summarized in Table I.

TABLE I - Position (in eV) of the main peaks in the absorption spectrum of aluminum from various sources.

Structures	Sagawa et al. ⁽⁹⁾	Fomichev ⁽¹⁰⁾	Codling ⁽¹⁰⁾	Haensel et al. ⁽¹⁰⁾	Gähwiler ⁽¹⁰⁾	Present work
L ₃	72.72	72.59	72.72	72.72	72.71	72.72
L ₂	73.16	73.02	73.15	73.15	73.15	73.10
e	81	84	84	84.3	85	83.3
f	87.4					90.6
g	96	96	96	97	97	96.6
h	110	110		113.5	112	108.5
L ₁	117	125	117	118	117.4	118
l	125	125		124	125	123
m	155					144
n	167	165		160	155	165
o						207

FIG. 11 - Transmission of indium and gold films in the spectral range 50-110 Å.

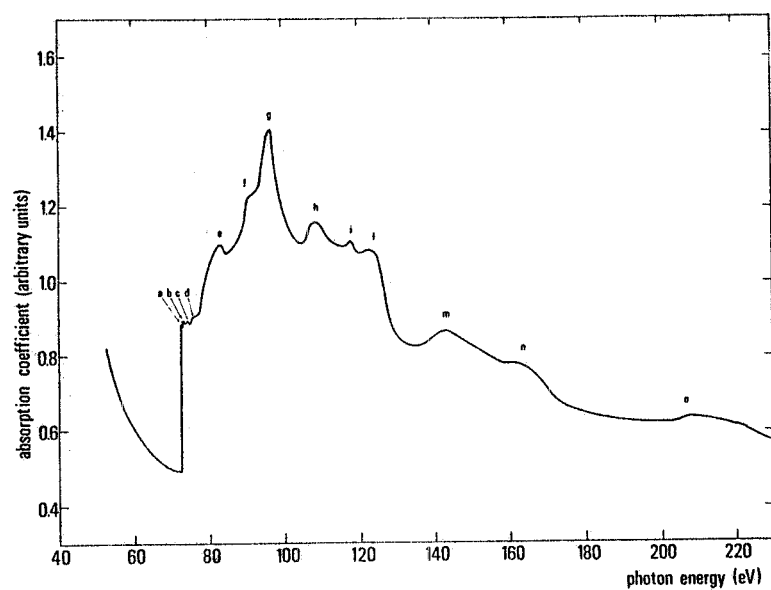
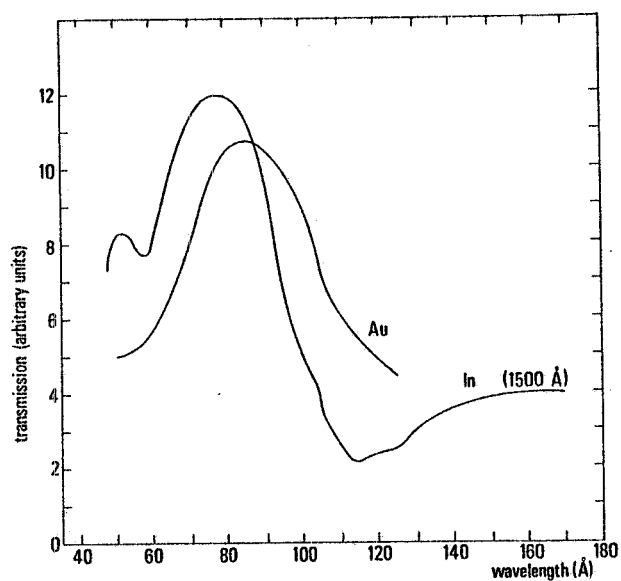


FIG. 12 - Absorption spectrum of an aluminum film.

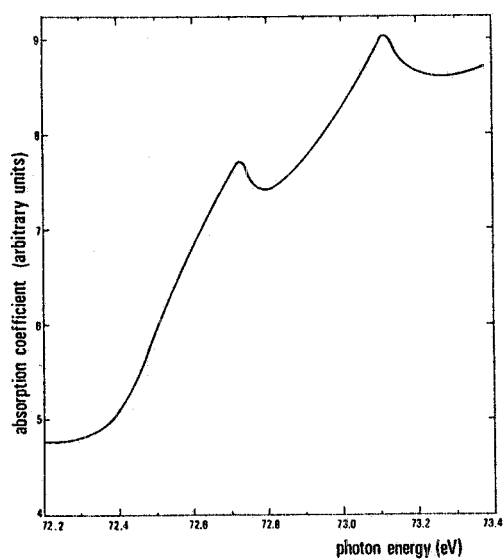


FIG. 13 - Absorption spectrum of an aluminum film in the region of the L₂, L₃ thresholds.

The shoulder at 90.6 eV, which is present in all our spectra, has been reported only by Sagawa et al.⁽⁹⁾. It should be noted that some peaks are better resolved than in previous investigations; the intense peak g looks sharper and the peak i at 118 eV, corresponding to the L_1 threshold, is clearly separated by its neighbors. In order to have additional evidence of the good quality of our apparatus, we have scanned across the absorption edge with great care and the result is shown in Fig. 13: the spin-orbit splitting of the L_2 - L_3 edges is well resolved, the separation being 0.38 ± 0.03 eV.

The authors are indebted to Prof. I. F. Quercia, Director of the Frascati National Laboratories, to Prof. G. F. Bassani and Prof. G. Chiarotti of the University of Rome and to Prof. D. Steve Boccia relli of the Istituto Superiore di Sanità for their continuous interest. They also acknowledge gratefully Mr. A. D'Innocenzo for his assistance during the measurements. They would like to thank the technicians M. Cinti, A. Maiolo, A. Mancini, and C. Ranghiasi for their invaluable help with the experimental apparatus. Thanks are also due to the technological group and to the Frascati accelerator staff, particularly Mr. A. Del Grande.

REFERENCES -

- (1) - R. P. Goodwin, Springer Tracts in Modern Physics, (Springer Verlag, 1969), vol. 51.
- (2) - 3rd Intern. Conf. on Vacuum Ultraviolet Radiation Physics Tokyo (1971), Published by Phys. Soc. of Japan.
- (3) - P. Jaeglè and G. Missoni, *Compt. Rend* 262, 71 (1966); P. Jaeglè, G. Missoni and P. Dhez, *Phys. Rev. Letters* 13, 337 (1967); P. Jaeglè, F. Combet Farnoux, P. Dhez, M. Cremonese and G. Onori, *Phys. Letters* 26 A, 364 (1968).
- (4) - A. Balzarotti, M. Piacentini, and M. Grandolfo, *Lett. Nuovo Cimento* 3, 15 (1970).
- (5) - A. Balzarotti, M. Grandolfo and M. Piacentini, ISS report 69/13 (1969).
- (6) - J. Schwinger, *Phys. Rev.* 75, 1912 (1949); A. A. Sokolov and J. M. Ternov, *Synchrotron radiation* (Akademic Verlag, 1968).
- (7) - Carbon films of different thicknesses were obtained by Yssum Research Development Comp., Hebrew University, Jerusalem, Israel.
- (8) - C. Gähwiller, F. C. Brown, and H. Fuyita, *Rev. Scient. Instr.* 41, 1275 (1970).

- (9) - T. Sagawa, Y. Iguchi, M. Sasanuma, A. Ejiri, S. Fujiwara, M. Yokota, S. Yamaguchi, M. Nakamura, T. Sasaki, and T. Oshio, *J. Phys. Soc. Japan* 21, 2602 (1966).
- (10) - V. A. Fomichev, *Fiz T ved. Tela* 8, 2892 (1967); *Soviet Phys. Solid State* 8, 2312 (1967); K. Codling and R. P. Madden, *Phys. Rev.* 167, 587 (1968); R. Haensel, C. Kunz, T. Sasaki and B. Sonntag, *J. Appl. Phys.* 40, 3046 (1969); C. Gähwiller and F. C. Brown, *Phys. Rev. B* 2, 1918 (1970); A. Ejiri, S. Yamaguchi, M. Saruwatari, M. Yokota, K. Inayoshi, and G. Matsuoka, *Opt. Comm.* 1, 349 (1970).